Structure and Dehydrogenation of the pure and Ti-doped (1 0 0) $KMgH_3$ surface

1. Introduction

Perovskite-type $KMgH_3$ is interesting as a potential hydrogen storage material because it is lightweight and has a high gravimetric hydrogen density [1] [2]. Recently, research on this hydride has focused on understanding its structure and stability. Reshak et al. reported computational results on one stable and two unstable phases, according to the location of the hydride ions, which is difficult to determine by experiment. The hydrogen bonds in the stable perovskite phase are ionic with potassium and slightly covalent with magnesium. In other hydrides of type AMgH$_3$, tilting of the MgH_6 octahedra has been observed, whereas this affect is less pronounced in $KMgH_3$ [2]. Since this tilting increases the difficulty of hydrogen diffusion within the bulk, $KMgH_3$ may have an advantage over other perovskite hydrides as a hydrogen storage material. Also, present studies disagree on the formation energy of $KMgH_3$, but all estimates are higher than the formation energy than MgH_2, which is known to be stable [2] [3] [4].

Studies on the kinetics of type AMgH$_3$ hydrides have revealed rapid hoping of H atoms within the bulk, compared to MgH_2 [4]. $NaMgH_3$ has displayed a lower dehydrating temperature than magnesium hydride, and is the hydrogenated product when Si-MgH_2-NaH is re-hydrogenated [4] [5]. So far, no information is available on the effect of metal dopants on the kinetics of type AMgH$_3$ hydrides. In MgH_2, bulk dopants such as niobium provide instant nucleation sites for Mg, through which metal diffusion of H atoms is accelerated [5] [6]. The probable rate limiting step for hydrogen release from MgH_2 is surface desorption [5] [7] [8], and metal doping on the surface of MgH_2 has improved hydrogen desorption [9]. Since hydrogen diffusion through the bulk of $KMgH_3$ is likely faster than in MgH_2, surface doping is likely the more effective method of lowering the dehydrogenation energy of $KMgH_3$.

To study the desorption of hydrogen from $KMgH_3$, this paper uses DFT to investigate titanium doped models of $KMgH_3$ and two reaction mechanisms that describe the formation of H_2 from Mg-H complexes in the (1 0 0) surface of $KMgH_3$. Sites favorable to Ti-doping are compared and evaluated according to the energies necessary for such doping; the stability of the Ti-doped structures are determined by their cohesive energies. Energy of dehydrogenation is used to compare desorption of hydrogen from doped and pristine models. It is found that Ti acts as a catalyst in $KMgH_3$, reducing the energy of dehydrogenation of the crystal surface. From the reaction mechanisms, it is suggested that the formation of Mg-Mg bonds on the surface may be precede H_2 desorption from the metal hydride.

2. Methodology

This project used generalized gradient approximation (GGA) calculations within the DFT formalism for the study of the structure, energetics, and dehydrogenation of pristine and modified potassium magnesium hydride. The PBE functional [10] and plane-wave basis (PW) set with valence electrons described by Vanderbilt ultra-soft pseudopotentials (USPP), were employed in all the calculations as implemented in the module CASTEP [11] of the Materials Studio software by Accelrys, Inc [12]. All calculations are performed spin-unpolarised.
The 0K energy of free neutral atoms and non-periodic molecules was found by geometry optimizing a single atom or molecule in a vacuum box of 10 x 10 x 10 Å. A medium k-point separation was used, as defined by the module, except with H_2, which was optimized with gamma k-point (calculated H-H bond length: 0.754 Å; 0 K energy: 31.699 eV). SFC convergence, with a plane-wave cutoff energy of 340 eV, was set at 2.0 x 10^{-6} eV/atom, except for Mg_2H_4 and Mg_2H_2-H_2, for which SCF converged to 1.0 x 10^{-6} eV/atom.
Geometry optimizations, electron density maps, and DOS plots were calculated for the pristine and doped models of $KMgH_3$, bulk metals, MgH_2 and KH with a medium k-point separation, a cutoff energy of 340

eV, convergence criteria set at 1.0 x 10^{-5} eV/atom, and a max force of 0.001 eV/ Å. Transition state searches followed a combined LST/QST procedure, with a RMS force convergence tolerance of 0.25 eV/ Å.Calculations and transition state searches for the products and reactants of proposed reaction mechanisms were preformed with a larger cutoff energy of 440 eV for greater accuracy.

3. Results

3.1 Structure of pristine KMgH₃

A potassium magnesium hydride unit cell (Figure 1a) wasmodeled according to its perovskite structure: space group Pm¯3mwith potassium, magnesium, and hydrogen atoms occupying the 1(*a*), 1(*b*) and 3(*c*) Wycoff positions, respectively [3]. The lattice parameters and bond lengths of the optimized unit cell (Table 1) are comparable with the experimental and theoretical values, respectively, reported by Reshak et al. [1]. The $KMgH_3$ electron density maps (Figure 1b) are also comparable to those obtained by Reshak et al., showing a high density around Mg compared to H and K (Figure 1b), and a spherical distribution around coordinated K and H atoms. The ionic character of the H-K interaction is greater than of the Mg-H bond in $KMgH_3$ [1] [2].The $KMgH_3$ total (TDOS) and partial (PDOS) density of states plots (Figure 1c) show slight H-s and Mg-p orbital hybridization in the valence band, although H-s account for the majority of states in the valence band. H and K orbitals do not interact significantly at any energy. The calculated band gap of the $KMgH_3$ cell is 2.487 eV, which is comparable to the theoretical values 2.32-2.6 eV reported by Reshak et al. [1].
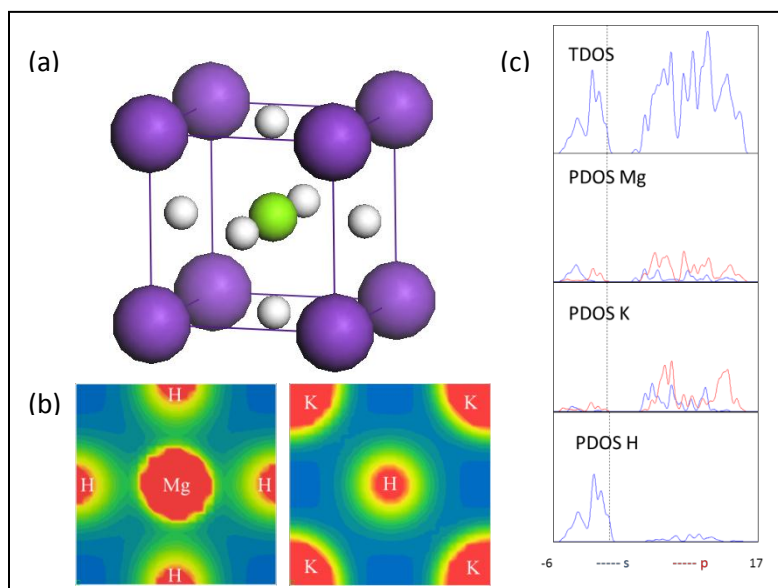

Figure 1. (a) The unit cell of $KMgH_3$, (b) its electron density along the (1 0 0) crystallographic plane, and (c) it TDOS and PDOS

Table 1.the Pm¯3m space group with potassium, magnesium, and hydrogen atoms occupying the 1(*a*), 1(*b*) and 3(*c*) Wycoff positions, respectively

	Calc. (Å)	Expt. (Å) [1]	Other Theoretical (Å) [1]
Lattice Parameters	*a* = *b* = *c* = 4.019	*a* = 4.023, 4.025	*a* = 4.035, 4.0295, 4.01

K-H	2.842	2.853, 2.85
K-Mg	3.481	3.495, 3.49
Mg-H	2.010	2.018
H-H	2.842	2.853

3.2 Structure of modified KMgH₃

To study Ti-dopant effects in the potassium magnesium hydride a bulkmodel (Figure 2a), a (1 0 0) Mg-terminated surface (Figure 2b) and a (1 0 0) K-terminated surface (Figure 2c) were constructed. A 2 x 2 x 2 supercell was optimized to simulate the $KMgH_3$ bulk.The (1 0 0) surface has a lower surface energy than the (1 1 0) and (1 1 1) surfaces and is symmetric to the (0 0 1) surface. The pure surface model was cleaved to have 4 layers, with a 9 Å vacuum slab extended in the "c" direction. To simulate the bulk below the surface, the two lowest surface layers were constrained. All bulk and surface models contain 8 $KMgH_3$ units (N = 40 atoms).The un-doped and doped models are considered in terms of bond lengths, TDOS, PDOS and cohesive (E_{coh}), substitution (ΔE_{subst}), titanium-addition (ΔE_{add}) and dehydrogenation energies. The energy calculations are governed by Equations 1-3.

$$\Delta E_{coh} = E_T(A_a B_b C_c \dots) - a\, E_T(A) - b\, E_T(B) - c\, E_T(C) - \cdots \quad (1)$$

The substitution energy per atom of X (= Mg or K, where the other = A) by Ti, ΔE_{subst}, is defined by Equation (3)

$$\Delta E_{subst} = \frac{E_{coh}(TiX_7 A_8 H_{24}) - E_{coh}(X_8 A_8 H_{24})}{N} \quad (2)$$

The titanium-addition energy per atom, ΔE_{add}, is defined by Equation (3)

$$\Delta E_{add} = \frac{E_{coh}(TiK_8 Mg_8 H_{24}) - E_{coh}(K_8 Mg_8 H_{24})}{N} \quad (3)$$

3.2.1 Bulk and surface models

Figure 2 shows the test sites where Ti was initially added in the doped models; in total 7 different models were considered. The models are described in Table 2. The optimized ground state conformations are shown in Figure 3, with the Ti-dopant colored red.

Table 2. Pristine and doped bulk and surface models

Model	Explanation
K → B$_K$	Pristine, bulk
Ti → B$_K$	Ti substituting K at K lattice site inside bulk
Mg →M$_{Mg}$	Pristine, Mg-terminated
Ti → M$_{Mg}$	Ti substituting Mg at Mg lattice site
Ti →M$_I$	Ti added to interstitial site between two Mg lattice sites in top layer
K → K$_K$	Pristine, K-terminated
Ti → K$_K$	Ti substituting K at K lattice site

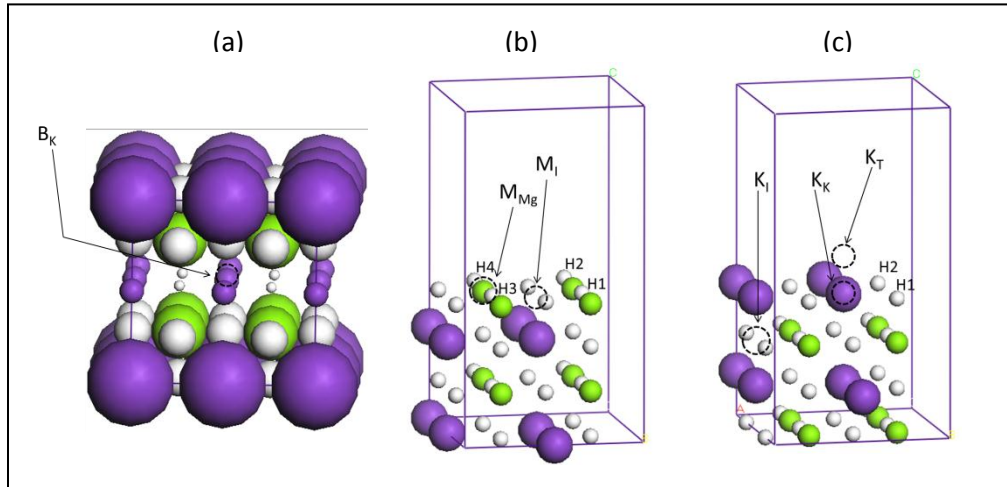|	
Ti → K$_I$	Ti added to interstitial site between two K lattice sites in between top and second layers
Ti → K$_T$	Ti placed on-top aK lattice site

Figure 2. Surface models and

The lattice structure is preserved with small changes in bond length in the optimized Ti-doped bulk model (Ti → B$_K$).The calculated H–Ti bond length is ~2.68 Å, which is 0.2 Å shorter than the corresponding Na–H in pristine potassium magnesiumhydrate. The native Mg-K bond length is 3.48 Å; however, when Na is substituted by Ti dopant Mg–K ranges from 3.46 - 3.55 Å. The new bond length, Ti-Mg, is 3.42 Å.The calculated H-Mg bond length, compared to the native bond length, is shortened .03 Å for H atoms near to the Ti dopant and is stretched .04 Å for the next nearest H atoms.

The Ti dopant at M$_{Mg}$ (Ti → M$_{Mg}$ model (Figure 3a)) settles in the test site M$_{Mg}$ forming bonds with hydrogen which are bonded in the pristine case with Mg. This creates little distortion in the crystal lattice: the H atoms interacting with Ti do not appreciably change their position in the lattice.In the optimized Ti → M$_I$ model (Figure 4b), the Ti dopant migrates to a spot ~1 Å above M$_I$ and coordinates to four H and four Mg atoms at 1.91 and 3.36 Å, respectively.

The Ti dopant at K$_K$ (Ti → K$_K$ model, Figure 4c) settles below the test site K$_K$and coordinates to four aluminum and eight hydrogen atoms at 2.96 and an average of 1.95 Å, respectively. In the optimized Ti → K$_I$ model (Figure 4d), the Ti dopant migrates to a position above K$_I$ and coordinates to three H and two aluminum atoms at distances in the 1.87–1.95Å ranges and at 2.79 Å, respectively. In both these cases, the K atom nearest to the Ti-dopant partially desorbs from the surface, possibly because the interaction between Ti and H disrupts the stability of the ionic interaction between K and H.

The Ti dopant on-top the surface K site (Ti → K$_T$ model, Figure 4e) migrates towards the surface during optimizationand after optimizationnearly rests in the K$_K$ site.In this case, the Ti coordinates to 4 H atoms at ~2.2 Å, which is .3 Å greater than the Ti-H bond length in TiH compounds such asTiH$_2$ [13], and does not indicate the formation of Ti-H bonds.

The DOS plots of models Ti → K$_K$ (Figure 4a), Ti → K$_I$ (Figure 4b), and Ti → M$_I$ (Figure 4c) (the models with the most structural change after doping) show that the Ti-d orbitals do not contribute greatly

in any of the models to the valence band. Instead, in each model the contribution of Ti to the DOS peaks at an energy that has a local maximum of Mg or K contribution to the DOS. The main features of the DOS plots of the doped models compared to the DOS plots of the pristine case are a shift in the Fermi level toward the conduction band, a widening of the valence band and a narrowing of the conduction band. From these considerations it may be assumed that Ti does not bond with H in these models, but instead interacts with Mg and K to lower the energy gap between Mg/K and H orbitals. This is a possible explanation for the change in dehydrogenation energy discussed later.

Cohesive energy calculations (Table 3) show Ti $\rightarrow K_K$, Ti $\rightarrow K_I$, Ti $\rightarrow M_{Mg}$ and Ti $\rightarrow M_I$ to be stable, having higher cohesive energies than the corresponding pristine $KMgH_3$ surface model. The energetically preferred doping sites are shown for both terminations of the surface by the substitution energy (Equation (1);Ti $\rightarrow K_K$ and Ti $\rightarrow M_{Mg}$ models) and titanium-addition energy(Equation (2); Ti $\rightarrow K_I$ and Ti $\rightarrow M_I$ models). Calculations show that the substitution/addition energies rank Ti $\rightarrow K_K \approx$ Ti $\rightarrow M_{Mg} <$ Ti $\rightarrow K_I$ < Ti $\rightarrow M_I$ (Table 3). The difference between the energy required for Ti $\rightarrow K_K$ and Ti $\rightarrow M_{Mg}$ is 0.005 eV/atom, and the difference between the interstitial dopant cases is .01 eV/atom.Since Ti $\rightarrow K_K$ and Ti $\rightarrow M_{Mg}$ require the least energy, K_K and M_{Mg} and possibly K_I would be preferred by a Ti dopant over M_I. M_I, however, is considered as a potential doping site because a difference of .03 eV/atom would be insignificant at fuel cell operating temperatures.
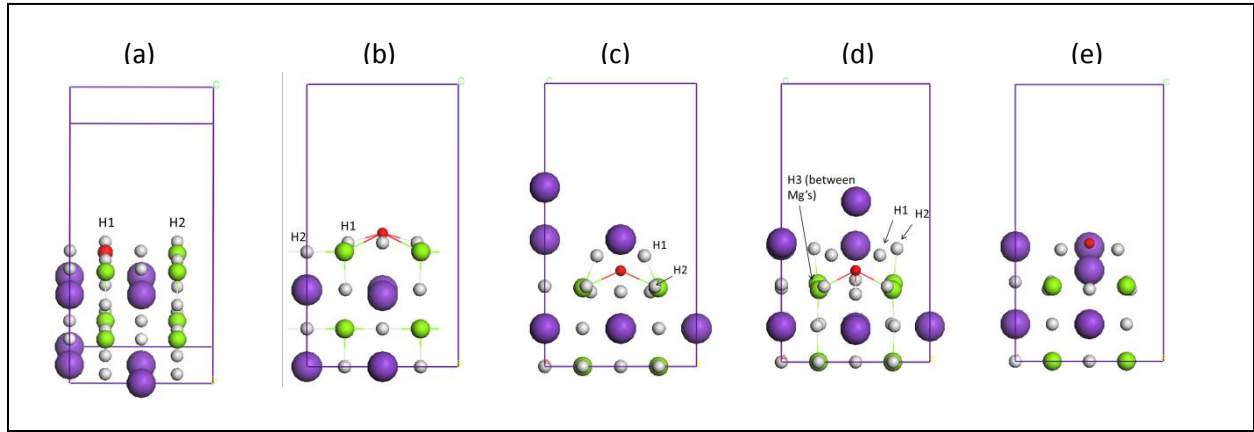

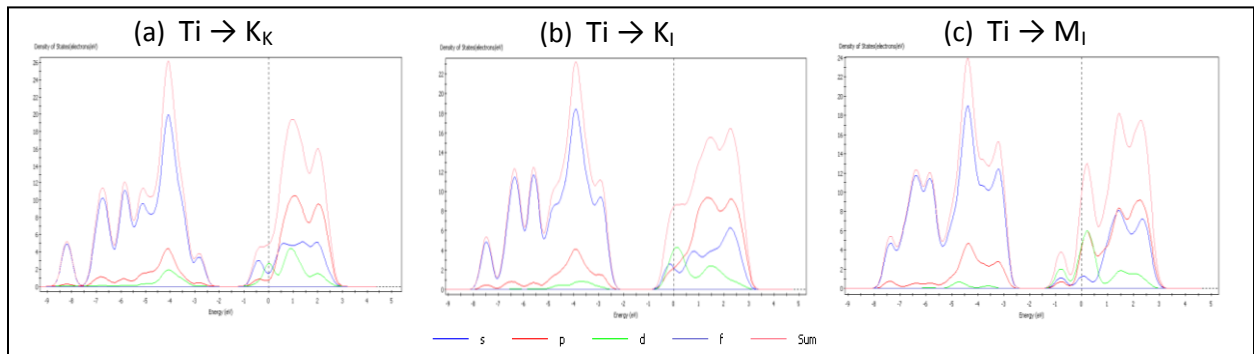Figure 3. Optimized Ti-doped models of the $KMgH_3$ (1 0 0) surface.

Figure 4. PDOS of selected Ti-doped models

Table 3. Cohesive energy relative to pristine system (for surfaces, relative to pristine K-terminated surface), E_{coh}*; Ti-addition energy, ΔE_{Ti}; and substitution energy (Ti $\rightarrow$ Mg or Ti $\rightarrow$ K), ΔE_{subst}

Site	Species in Site	System	E_{coh}* (eV)	ΔE_{Ti} (eV/atom)	ΔE_{subst} (eV/atom)

B$_K$	K	K$_8$Mg$_8$H$_{24}$	0.00		
	Ti	TiK$_7$Mg$_8$H$_{24}$	-0.07		-0.002
K$_K$	K	K$_8$Mg$_8$H$_{24}$	0.00		
	Ti	TiK$_7$Mg$_8$H$_{24}$	3.12		0.078
K$_I$	Ti	TiK$_8$Mg$_8$H$_{24}$	3.84	0.096	
K$_T$	Ti	TiK$_8$Mg$_8$H$_{24}$	-1.66	-0.042	
M$_{Mg}$	Mg	K$_8$Mg$_8$H$_{24}$	0.15		
	Ti	TiK$_8$Mg$_7$H$_{24}$	3.07		0.073
M$_I$	Ti	TiK$_8$Mg$_8$H$_{24}$	4.35	0.105	

3.2.4 Dehydrogenation energy

In order to investigate the effect of Ti-doping on the suitability of KMgH$_3$ for hydrogen storage, the dehydrogenation energies of the pristine and doped surfaces were found. This was done by deleting H atoms from the surface and comparing the 0K energy (without ZPE) of the optimized resulting structure to the energy of the complete surface, according to Equation (4)

$$\Delta E_{dehyd} = E_T(Ti_x K_y Mg_z H_{24}) - [\, E_T(Ti_x K_y Mg_z H_{24-a}) + \frac{a}{2} E_T(H_2)\,]\ (4)$$

where x, y, and z change with the surface and a is the number of H atoms removed. Results are shown in Table 4.

The dehydration energy changed most dramatically in the Ti $\rightarrow$K$_I$ model: depending on the H atom considered the dehydration energy decreased by 80.7-88.8 kJ/mol H with the substitution of Ti for K. All Ti doped models exhibited lower dehydrogenation energies than the corresponding pristine models. In general, the K-terminated surface and doped models exhibited lower dehydrogenation energy than the Mg-terminated surface. This can be understood as a result of stronger interactions between the H and Mg atoms than between H and K atoms, as was suggested by the DOS analysis.

By removing a pair of hydrogen atoms from the pristine models and bringing the atoms within a H$_2$ bond length of each other in the vacuum above, the product of a dehydrogenation reaction was simulated for both pristine models. Using this as the product and the pristine model as the reactant, the transition state search functionality of the CASTEP module estimated the activation energy of releasing H$_2$ from the pure KMgH$_3$ surface to be 244.1 and 282.7 kJ/mol H$_2$, for K- and Mg-terminated surfaces respectively.

Table 4. Dehydrogenation energy (E$_{dehyd}$) for removing H atoms from pristine and doped surfaces and the activation barrier (E$_a$) for H$_2$ desorption

Model (x, y, z)	H atoms removed	H bonds broken	E$_{dehyd}$ (kJ/a mol H)	E$_a$ (kJ/mol H$_2$)
K-terminated (0,8,8)	H1	Mg-H	118.971	
	H1, H2	2 Mg-H	214.935	244.118
Ti $\rightarrow$K$_K$ (1,7,8)	H1	Ti-H, Mg-H	53.415	
	H2	Ti-H	33.976	
Ti $\rightarrow$K$_I$ (1,8,8)	H1	Ti-H	30.172	
	H2	Mg-H	30.796	
	H3	2 Mg-H	38.282	
Mg-terminated (0,8,8)	H1	2 Mg-H	130.144	
	H1, H2	4 Mg-H	162.316	282.702

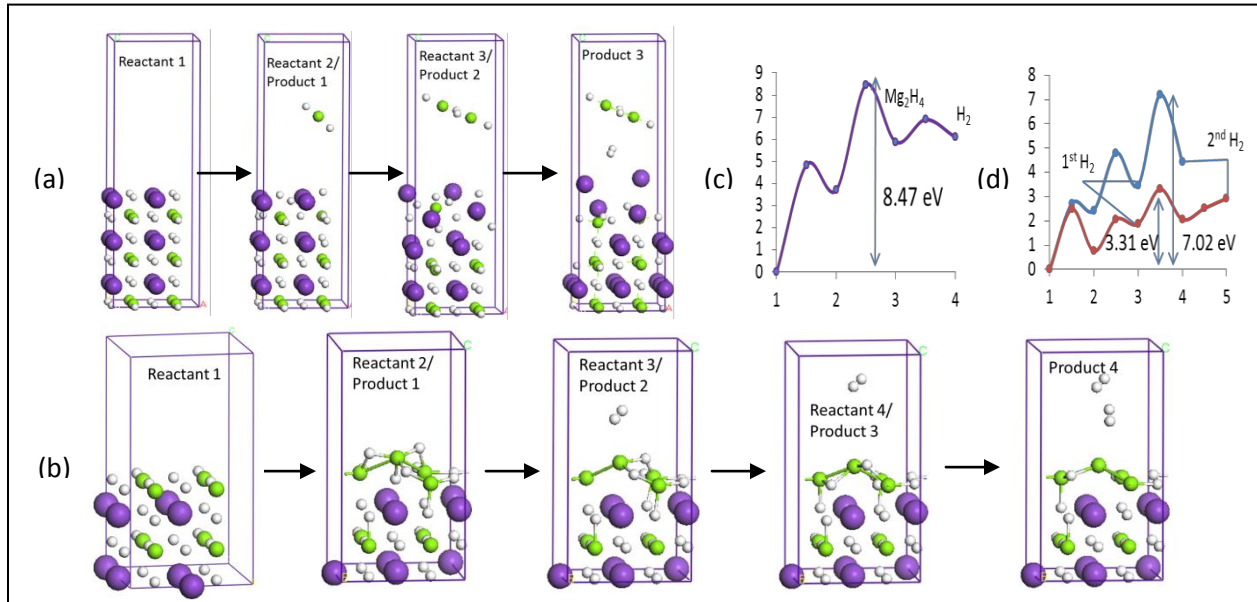|	H1-4		309.847
Ti →M_{Mg} (1,8,7)	H1	Ti-H, Mg-H	121.739
	H2	2 Mg-H	84.961
Ti → M_I (1,8,8)	H1	Ti-H, 2 Mg-H	56.673
	H2	2 Mg-H	72.702

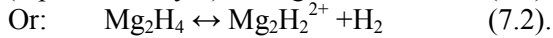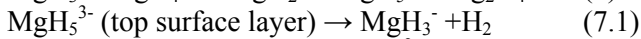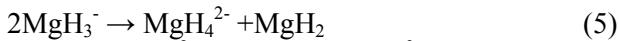## 3.3 Dehydrogenation reaction path

Figure 5.

In an attempt to understand the kinetics of hydrogen desorption from the (1 0 0) $KMgH_3$ surface, two separate reaction mechanisms were considered, and models were constructed to test the energy path for each mechanism. The first mechanism follows Equations (5)-(6) and (7.1) or (7.2)

$$2MgH_3^- \rightarrow MgH_4^{2-} + MgH_2 \quad (5)$$
$$MgH_3^- + MgH_4^{2-} + MgH_2 \leftrightarrow MgH_5^{3-} + Mg_2H_4 \quad (6)$$
$$MgH_5^{3-} \text{ (top surface layer)} \rightarrow MgH_3^- + H_2 \quad (7.1)$$
$$\text{Or:} \quad Mg_2H_4 \leftrightarrow Mg_2H_2^{2+} + H_2 \quad (7.2).$$

To model these reactions, a new K-terminated surface was cleaved from a 2 x 2 x 3 bulk cell, resulting in a 6-layer surface with a 15 Å vacuum slab extended in the c direction. The release of MgH_2 from the lattice structure (either by desorption or diffusion) is modeled by removing an Mg and two nearby H atoms from the lattice and placing the resulting MgH_2 molecule (Mg constrained) in the vacuum (Figure 5a, Reactant 1 → Product 1). Reaction (6) is modeled similarly, with a pre-optimized Mg_2H_4 molecule fully constrained in the vacuum of the product model (Figure 5a, Reactant 2→ Product 2). Reaction (7.1) is modeled in the product stage by constraining a pre-optimized Mg_2H_2 molecule in the vacuum and by bringing two H atoms in vacuum to a distance equal to the DFT calculated bond length of H_2 (Figure 5a, Reactant 3 → Product 3.1). Reaction (7.2) is modeled in the product stage by moving two H atoms formally in the in MgH_5^{3-}complex into the vacuum to a distance equal to the DFT calculated bond length of H_2 (Figure 4a, Reactant 3 → Product 3.2). Transition states between Reactants and Products (1), (2), (3 → 3.1) and (3 → 3.2) are located using LST/QST procedure as implemented in the TS search function of

the CASTEP module. The energy path of the reaction mechanism (Figure 6a) is given in terms of total 0K energy, relative to the pure surface.

The second reaction mechanism involves the formation of an Mg-H complex in the highest Mg layer. A minimum in the potential energy surface was found for both K- and Mg-terminated surfaces when a single Mg atom is outside its native lattice site. In both cases the Mg atom settles above the nearest K in the layer below and slightly above the plane of the atom's original layer. Since these two cases are similar, only one is shown (Figure 5b, Product 1). The shifted Mg atom coordinates to three Mg atoms in the layer at 2.9-3.5 Å. Since in DFT optimized Mg(-H) structures such as Mg (metal), MgH_2 (crystal), and Mg_2H_4 (molecule) the Mg-Mg coordination is 3.2, 3.5 and 2.8 Å respectively, the modified structure likely contains Mg-Mg bonds. From these modified structures, the release of H_2 is simulated by moving two H atoms previously bonded to the shifted Mg into the vacuum close enough to bond (Figure 5b, Product 2). The release of a second H_2 is simulated by moving 2 H atoms from Product 2 – one bonded to an outside Mg and the other bonded to the center Mg – into the vacuum close enough to bond (Figure 5b, Product 4). Because of the large activation energy calculated for Reactant 2 → Product 2, an intermediate step was introduced in the Mg-terminated case, where the H atom bonded to the outside Mg first diffuses to the vacant site near the center Mg atom before bonding with the other H atom above the surface. This energy path of this reaction (Figure 5c, Reactant 2 → Product 2/Reactant 3 → Product 3) has a much smaller overall energy barrier.

The plots of the total energy of reactions 1 and 2 relative to the first step are shown in Figure 5c and 5d respectively.

To determine whether this final geometry, with Mg out of its original lattice site after dehydrogenation, would be preferred to the original geometry, two Mg-terminated surface models were constructed. H_2 was removed from one and $2H_2$ from the other. After optimization, the Mg atoms had moved closer to one another where H atoms had been removed, but none had migrated out of the layer plane. The 0K energy of the model with H_2 was .40 eV lower than that of Product 1 (Mg), but that of the model with $2H_2$ was .14 eV higher than Product 3 (Mg). This may show that the perovskite structure of $KMgH_3$ becomes less stable than the metallic Mg phase before full dehydrogenation. More investigations of mechanisms such as the one described are necessary to understand when this change occurs.

4. Discussion/Conclusion

This study concludes from DFT simulations that titanium improves the dehydrogenation energy of the (1 0 0) $KMgH_3$ surface. Four locations were found that Ti can occupy on this surface that result in a stable structure – relative to the pure surface – based on the cohesive energies of the resulting structure. Other possible locations that were not considered are interstitial or substituting sites in lower layers. Ti $\rightarrow M_{Mg}$ was the only stable model that when optimized did not form a Ti-Mg complex, and its dehydrogenation energy was the highest observed of the doped models. Therefore, in $KMgH_3$, single transition-metal atom dopants likely affect dehydrogenation by forming Ti-Mg complexes.

In the models that did form Ti-Mg complexes, the DOS plots show that Ti electrons were not abundant in the valence band compared to the conduction band. However a correlation is seen between the contribution of Ti to the valence band and the dehydrogenation energy of the model. The height of the tallest Ti-d peak in the valence band varied with the model, according to the following ranking: Ti-d peak height in Ti $\rightarrow K_K$ > in Ti $\rightarrow K_I$ > in Ti $\rightarrow M_I$. The dehydrogenation energy of these models decreased in reverse order: E_{dehyd} Ti $\rightarrow K_K$ < Ti $\rightarrow K_I$ < Ti $\rightarrow M_I$. Because of this correlation, the presence of electrons from the dopant d-orbitals in the valence band could be used to compare the effect of different transition metal dopants on the $KMgH_3$ surface, when those dopants form complexes with magnesium.

Of the two dehydrogenation reactions studied, the reaction which formed an Mg complex in the top magnesium layer showed activation barriers closest to those observed when removing hydrogen from the pure surface. Also, the total energies of the pure and modified surface after dehydrogenation were similar. The activation barrier for the formation of the magnesium complex, at least in the Mg-terminated model of the surface, was smaller than the activation barrier for H_2 release. Therefore, if a magnesium complex like the one observed is stable at high temperatures, it is likely that the nucleation of magnesium on the surface of $KMgH_3$ precedes H_2 release in a dehydrogenation reaction. This is perhaps consistent with the fact that hydrogen mobility in magnesium hydride is limited until the magnesium nucleates to form a metallic phase [5] [6]. In MgH_2 this is a bulk phenomenon; in future studies, the nucleation of magnesium in the $KMgH_3$ bulk could be studied for comparison with MgH_2, considering that doping MgH_2 has made nucleation of magnesium almost instantaneous [6].

The possible dehydrogenation reaction which involved the diffusion of Mg_2H_4 proved to be very energetically unfavorable. The highest activation barrier to a single step occurred when an Mg atom was simulating diffusing from the surface, and in terms of total energy, the bonding of the Mg atoms in the vacuum only released half the energy necessary to remove the second Mg atom from the surface. Also considering that the activation energy of releasing hydrogen from the pure surface was a half of that of releasing magnesium, it is unlikely that desorption of magnesium complexes will aid the dehydrogenation kinetics of $KMgH_3$. Nevertheless, the local displacement of an MgH_2 group, perhaps to a nearby layer, was not studied in this project and may still yield a favorable path, since the desorption of H_2 from the surface without Mg_2H_4 was favorable.

5. References

[1] Reshak, A.H., Shalaginov, M.Y., Saeed, Y., Kityk, I.V., Auluck, S. "First-principles calculations of structural, elastic, electronic, and optical properties of perovskite-type KMgH3 crystals: Novel hydrogen storage material." Journal of Physical Chemistry B, Volume 115, Issue 12, 31 March 2011, Pages 2836-2841

[2] M. Fornari, A. Subedi, and D. J. Singh. "Structure and dynamics of perovskite hydrides AMgH3 (A=Na, K, Rb) in relation to the corresponding fluorides: A first-principles study." Physical Review B - Condensed Matter and Materials Physics. Volume 76, Issue 21, 27 December 2007, Article number 214118

[3] Klaveness, A., Swang, O., Fjellvag, H. "Formation enthalpies of NaMgH3 and KMgH3: A computational study." Europhysics Letters. Volume 76, Issue 2, 15 October 2006, Pages 285-290

[4] Wu, H., Zhou, W., Udovic, T.J., Rush, J.J., Yildirim, T. "Crystal Chemistry of Perovskite-Type Hydride NaMgH3: Implications for Hydrogen Storage." Chemistry of Materials. Volume 20, Issue 6, 25 March 2008, Pages 2335-2342

[5] Schimmel, H.G., Huot, J., Chapon, L.C., Tichelaar, F.D., Mulder, F.M. "Hydrogen Cycling of Niobium and Vanadium Catalyzed Nanostructured Magnesium." Journal of the American Chemical Society. Volume 127, Issue 41, 19 October 2005, Pages 14348-14354

[6] Bazzanella, N., Checchetto, R., Miotello, A. "Atoms and Nanoparticles of Transition Metals as Catalysts for Hydrogen Desorption from Magnesium Hydride." Journal of Nanomaterials. Volume 2011, 2011, Article number 865969

[7] Du, A.J., Smith, S.C., Lu, G.Q. "First-principle studies of the formation and diffusion of hydrogen vacancies in magnesium hydride." Journal of Physical Chemistry C. Volume 111, Issue 23, 14 June 2007, Pages 8360-8365

[8] Wu, G., Zhang, J., Li, Q., Wu, Y., Chou, K., Bao, X. "Dehydrogenation kinetics of magnesium hydride investigated by DFT and experiment." Computational Materials Science. Volume 49, Issue 1 SUPPL., 2010, Pages S144-S149

[9] Dai, J.H., Song, Y., Yang, R. "First Principles Study on Hydrogen Desorption from a Metal ()Al, Ti, Mn, Ni) Doped MgH2 (110) Surface." Journal of Physical Chemistry C. Volume 114, Issue 25, 1 July 2010, Pages 11328-11334

[10] J.P. Perdew and Y. Wang, Accurate and simple analytic representation of the electron-gas correlation energy, Phys. Rev. B 45 (1992), pp. 13244–13249

[11] M.D. Segall et al., First-principles simulation: ideas, illustrations and the CASTEP code, J. Phys. Cond. Matt. 14 (2002), pp. 2717–2743

[12] Accelrys, Materials Studio (2006).

[13] Dathara, G.K.P., Mainardi, D.S. "Structure and dynamics of Ti-Al-H compounds in Ti-doped NaAlH4." Molecular Simulation. Volume 34, Issue 2, February 2008, Pages 201-210